Petroleomic Depth Profiling of Staten Island Salt Marsh Soil: 2ω Detection FTICR MS Offers a New Solution for the Analysis of Environmental Contaminants

Mary J. Thomas[a,b], Emma Collinge[b], Matthias Witt[c], Diana Catalina Palacio Lozano[b,d], Christopher H. Vane[e], Vicky Moss-Hayes[e] and Mark P. Barrow[b*]

[a]*MAS CDT, Senate House, University of Warwick, Coventry, CV4 7AL, UK*

[b]*Department of Chemistry, University of Warwick, Coventry, CV4 7AL, UK*

[c]*Bruker Daltonik GmbH, Bremen, 28359, Germany*

[d]*Facultad de Ciencias, Universidad Industrial de Santander, Bucaramanga, Colombia*

[e]*British Geological Survey, Centre for Environmental Geochemistry, Keyworth, NG12 5GG, UK*

Email: m.thomas.6@warwick.ac.uk, E.Collinge@warwick.ac.uk, Matthias.Witt@bruker.com, D.Palacio-Lozano@warwick.ac.uk, chv@bgs.ac.uk, vmh@bgs.ac.uk, M.P.Barrow@warwick.ac.uk

*Corresponding Author

ABBREVIATIONS

Atmospheric pressure chemical ionization (APCI)

Atmospheric pressure photoionization (APPI)

Direct infusion (DI)

Double bond equivalents (DBE)

Extracted ion chromatogram (EIC)

Gas chromatography (GC)

Fourier transform ion cyclotron resonance mass spectrometry (FTICR MS)

ABSTRACT

Staten Island is located in one of the most densely populated regions of the US: the New York/New Jersey Estuary. Marine and industrial oil spills are commonplace in the area, causing the waterways and adjacent marshes to become polluted with a range of petroleum-related contaminants. Using Rock-Eval pyrolysis, the hydrocarbon impact on a salt marsh was assessed at regular intervals down to 90 cm, with several key sampling depths of interest identified for further analysis. Ultrahigh resolution data are obtained by direct infusion (DI) atmospheric pressure photoionization (APPI) on a 12 T solariX Fourier transform ion cyclotron resonance mass spectrometer (FTICR MS) allowing trends in the compositional profile with depth to be observed, such as changes in the relative hydrocarbon intensity and the relative contributions from oxygen- and sulfur-containing groups. These trends may correlate with the timing of major oil spills and leaks of petroleum and other industrial chemicals into the waterways. The use of gas chromatography (GC) coupled to a 7 T solariX 2XR FTICR MS equipped with an atmospheric pressure chemical ionization (APCI) ion source offers retention time resolved and extensive compositional information for the complex environmental samples

complementary to that obtained by DI-APPI. The compositional profile observed using GC-APCI FTICR MS includes contributions from phosphorous-containing groups, which may be indicative of contamination from other anthropogenic sources.

KEYWORDS

Oil spill; soil contamination; Fourier transform ion cyclotron resonance; mass spectrometry; environmental monitoring

1. INTRODUCTION

New York/New Jersey (NY/NJ) Estuary supports one the highest population densities in the United States, consequently the shores of one of its main shipping channels, the Arthur Kill, hosts numerous waste generating industries. The NY/NJ Estuary was ranked among the most chemically contaminated waterways in the United States based on surface sediment concentrations and frequency of accidental chemical discharge events (Gunster, 1993; Packer, 1991). Elevated body burdens of toxic substances including heavy metals, petroleum hydrocarbons, and aromatic hydrocarbons have been detected in a wide range of aquatic wildlife (Packer 1991). Analysis of the spatial and down-core extent of contamination from anthropogenic sources including petroleum, industrial and agricultural chemicals, in estuarine and coastal regions is of rising importance due to increased demand on below ground space,

65 which may contain historic pollution, as well as greater understanding of the long term impact
66 on eco-system health (da Silva and Bicego, 2010; Langston et al., 2012; Oros and Ross, 2004;
67 Vane et al., 2008; Vane et al., 2009; Vane et al., 2011; Vane et al., 2018).

68 Environmental samples, particularly those contaminated with petroleum-related substances,
69 are highly complex, containing many thousands of components (Alimi et al., 2003; Richardson
70 and Ternes, 2018; Vane et al., 2018; White et al., 2013). The characterization of petroleum-
71 related samples using mass spectrometry has been termed 'petroleomics', with the molecular
72 formulae of tens of thousands of components observed in a single spectrum (Barrow, 2010;
73 Hsu et al., 2011). Petroleomics typically utilizes state-of-the-art, high field FTICR
74 instrumentation (Cho et al., 2015; Marshall et al., 2010) which offers ultrahigh resolution and
75 sub-ppm mass accuracy. However, these instruments are typically expensive to obtain and
76 maintain, as well as requiring expert operation. solariX 2XR FTICR MS instruments can
77 operate in a mode where ion detection occurs using 4 cell plates, compared to the usual 2, and
78 as such are able to detect at twice the usual frequency (Cho et al., 2017; Schweikhard et al.,
79 1990). 2ω detection allows for significant improvements in performance compared to other
80 FTICR instrumentation operating at the same field (Pan, 1988), specifically doubling
81 resolution for a set acquisition time or else offering equivalent resolution in half the time
82 (Schweikhard, 1991). The latter makes the technique well suited to hyphenated techniques,
83 including gas chromatography (GC), where a fast scan rate is required to maintain pace with
84 rapidly eluting components (Beens and Brinkman, 2000; Tessarolo et al., 2014; Wang et al.,
85 1997).

86 7 T FTICR instrumentation equipped with the option of 2ω detection has already demonstrated
87 ultrahigh resolution analytical capabilities in the analysis of petroleum samples (Cho et al.,
88 2017), offering equivalent performance at a lower magnetic field than previously required.

89 This, in turn, reduces the entry cost of FTICR MS for petroleomics and environmental analyses;
90 a 7 T instrument equipped with 2ω detection possesses performance capabilities comparable
91 to a 15 T instrument operating under the traditional conditions of detection at ω. 2ω detection
92 affords the ability to operate an FTICR mass spectrometer at twice the speed for the same
93 resolving power, which is useful for coupling with chromatography, or to operate at the same
94 speed but double the resolving power. Orbitrap MS instrumentation has also been used for
95 environmental analyses when coupled to prior chromatographic separation (Pereira and Martin,
96 2015), however FTICR MS remains most capable when handling ultra-complex samples. One
97 of the advantages of the ParaCell (Boldin and Nikolaev, 2011; Jertz et al., 2015) in solariX XR
98 and 2XR instruments is the ability to excite ions to a larger orbit radius than the Infinity Cell
99 design, which in turn yields greater signal-to-noise and reduction in space-charge effects (Cho
100 et al., 2017). Here, the application is extended to environmental samples, where coupling GC
101 can increase the scope of analysis to include the observation of multiple isomers for a single
102 molecular formula (Blomberg et al., 2002; Lalli et al., 2017; Schwemer et al., 2015), and to
103 provide an additional dimension of separation, aiding in the detection of low abundance species
104 (Schwemer et al., 2015).

105 Analyses of environmental samples including oil sands process-affected water (Barrow et al.,
106 2010; Headley et al., 2011), and soil from coastal regions affected by the Deepwater Horizon
107 spill (Chen et al., 2016) by direct infusion (DI) into FTICR MS instrumentation have been
108 successful. Coupling of chromatographic methods with FTICR MS has also been successfully
109 applied to the characterization of petroleum-contaminated soil (Zubair et al., 2015) and
110 weathered crude oils (Rowland et al., 2014). A range of ionization methods are available,
111 including electrospray ionization (ESI), laser desorption ionization (LDI), atmospheric
112 pressure photoionization (APPI), and atmospheric pressure chemical ionization (APCI), the
113 choice of which influences the observed profile (Barrow et al., 2010; Cho et al., 2013; Huba et

al., 2016). APPI preferentially accesses non-polar, conjugated systems, and produces both protonated and radical ion species, adding to spectral complexity (Cho et al., 2015) while atmospheric pressure chemical ionization APCI accesses both non-polar and polar compounds (Andrade et al., 2008). Coupling prior separation techniques, including GC, has been shown to add a further dimension of separation and improve the range of compounds observed by FTICR methods and to provide information on the range of isomers for each unique molecular formula assigned (Benigni et al., 2016).

In this study, the shallow salt marsh sediment core from Staten Island, New York, was sampled at 47 intervals to correlate the compositional fingerprints of the petroleum extracts with the history of oil spills this area. Rock-Eval(6) pyrolysis, a geochemical screening technique widely applied to the hydrocarbon bearing source rocks, was used as bulk geochemical reconnaissance method (Könitzer et al., 2016; Slowakiewicz et al., 2015). Rock-Eval generates parameters for total organic carbon (TOC), free hydrocarbons (S1), and bound (polymeric) hydrocarbons (S2). S1 describes the quantity and proportion of volatile hydrocarbons (free oil) S2 the bound hydrocarbons (biopolymers and kerogen). The production index is used as a benchmark for thermal maturity and calculated by dividing the amount of volatile hydrocarbons by total volatile and bound hydrocarbon (S1/S1+S2). In petroleum geochemistry resource assessment studies, immature rocks have a ratio of 0.1 or less, mature samples yield values of 0.1-0.4, and when expulsion occurs the S1 no longer rises (Pharaoh et al., 2018; Slowakiewicz et al., 2015).

In parallel to Rock–Eval pyrolysis screening geochemistry, solvent extracts were profiled using two instruments in different laboratories: DI-APPI FTICR MS using a solariX and GC-APCI FTICR MS using a solariX 2XR. The GC-APCI experiments were performed to access additional species, particularly more volatile components, and provide insight on the isomeric complexity of the extracts. An ultrahigh resolution mass spectrometer coupled with GC affords

the ability to accurately monitor signal intensities within very narrow *m/z* windows, including co-eluting components. By following the extracted ion chromatograms (EICs) in a manner not possible with lower resolution instrumentation including time-of-flight and quadrupole mass spectrometers, it is possible to obtain information about the range of isomers present for a single molecular formula (Barrow et al., 2014).

The detailed molecular characterization obtained by DI-APPI FTICR MS (solariX) and GC-APCI FTICR MS (solariX 2XR), along with the bulk information determined by Rock-Eval pyrolysis, allows a fingerprint of the anthropogenic contaminants of soil to be developed. Petroleomic profiles of soil as a function of depth can be used for correlating contamination with the site history, and may be developed as a tool for understanding the impact of oil and chemical spills in areas with a high concentration of industrial and shipping activity, for example.

2. MATERIALS AND METHODS

2.1 SEDIMENT SAMPLING

A sediment core was collected using an Eijkelkamp peat sampler fitted with a stainless steel gauge (50 cm × 5.2 cm i.d.) at 40 36 27.87912 N, 74 11 27.50687 W (± 5 m) from intertidal zone of Saw Marsh Creek, Staten Island, New York, USA on June 10th 2013 (Figure 1). Recovered core sections were stored in pre-cut clean UPVC pipe and transported in a cool box at approximately 4 °C and then frozen at -18 °C. Each core was sectioned continuously at 2 cm intervals up to and including 46 cm depth and at 1 cm up to 51.5 cm depth and then at 2 cm intervals to core base at 90 cm. All sediment intervals were then freeze-dried for 72 h, sieved through a mesh aperture of 2 mm and the < 2 mm fraction ground to a fine powder (Beriro et al., 2014; Vane et al., 2007).

Figure 1. Sampling location of Core.

2.2 ROCK-EVAL(6) PYROLYSIS

Forty seven depth increments from the Saw Marsh Creek core were analyzed using a Rock-Eval(6) pyrolyser. Powdered samples (60 mg dry wt.) were heated from 300 °C to 650 °C at 25 °C min^{-1} in an inert atmosphere of N_2 and the residual carbon then oxidised by the addition of a constant flow of clean compressed oxygen-containing air at 300 °C to 850 °C at 20 °C

172 min^{-1} (hold 5 min) . Hydrocarbons released during the two-stage pyrolysis were measured using
173 a flame ionization detector and CO and CO_2 measured using an IR cell. The performance of
174 the instrument was checked every 10 samples against the accepted values of the Institut
175 Français du Pétrole (IFP) standard (IFP 160 000, S/N1 5-081840). Rock-Eval parameters were
176 calculated by integration of the amounts of HC (thermally-vaporized free hydrocarbons)
177 expressed in mg HC^{-1} g^{-1} rock (S1) and hydrocarbons released from cracking of bound organic
178 matter (OM) expressed in mg HC^{-1} g^{-1} rock (S2). The production index is given by S1/S1+S2.

179 *2.3 SOXHLET EXTRACTION*

180 Environmental Protection Agency method 3540c was followed for 5 depth samples. 190 mL
181 dichloromethane (DCM) (Fisher Scientific, Hemel Hempstead, Hertfordshire, UK) was added
182 to each sample and heated at ~40 °C for 22 h to maximise the extraction of hydrophobic
183 components including petroleum-related compounds. The extracts were then cooled before
184 being evaporated under reduced pressure to 10 mL.

185 *2.4 DIRECT INFUSION (DI) APPI FTICR MS*

186 Extracts for 5 depths were diluted in dichloromethane (DCM) (Fisher Scientific, Hemel
187 Hempstead, Hertfordshire, UK) before mass spectra were acquired using a 12 T solariX FTICR
188 mass spectrometer (Bruker Daltonik GmbH, Bremen, Germany), coupled to an APPI II source.
189 The instrument was operated in positive-ion mode. Nitrogen was used as the drying gas at a
190 temperature of 200 °C at a flow rate of 4 L min^{-1}. The nebulizing gas was nitrogen and was
191 maintained at a pressure of 1.0 bar. Samples were infused using a syringe pump at a rate of 750
192 µL h^{-1} without the activation of in-source dissociation. 4 MW data sets were acquired using
193 magnitude mode, with a detection range of *m/z* 98-3000. After acquiring 300 scans, the data
194 were zero-filled once and apodized using a Sine-Bell function prior to applying a fast Fourier
195 transform. For the apodized data, the measured resolving power at *m/z* 200 was 650,000. Data

were internally calibrated using homologous series (Table S1) and analyzed using DataAnalysis 4.2 (Bruker Daltonik GmbH, Bremen, Germany). Assignments were made using Composer 1.5.7 (Sierra Analytics, Modesto, CA, USA), searching for homologous series within the elemental constraints C=0-200; H=0-1000; N=0-2; O=0-9; S=0-2; P=0-1 (Table S2). Aabel NG2 v.5.2 (Gigawiz Ltd. Co., Tulsa, Oklahoma, USA) was used for data visualization.

2.5 GC-APCI FTICR MS

Extracts for 4 depths were diluted in DCM (Sigma Aldrich Chemie GmbH, Munich, Bavaria, Germany). Mass spectra were acquired using a 7 T solariX 2XR FTICR mass spectrometer (Bruker Daltonik GmbH, Bremen, Germany), coupled to a GC 450 (Bruker Daltonik GmbH, Bremen, Germany) and GC-APCI II source. 1 µL injection volume onto a 30 m BR-5ms column was used with He as the carrier gas, with the temperature program as follows: 60 °C held for 1 min, ramping 6 °C min^{-1} up to 300 °C and held for 9 min. The instrument was operated in positive-ion mode. Nitrogen was used as the drying gas at a temperature of 240 °C at a flow rate of 4 L min^{-1}. The nebulizing gas was nitrogen and was maintained at a pressure of 2.0 bar. 2 MW data sets were acquired using magnitude mode, with a detection range of *m/z* 107-3000 and 95 % data profile reduction. 2ω (quadrupolar) detection was used, affording high resolution at the rapid scan rate required for GC-APCI infusion. The data were zero-filled once and apodized using a Sine-Bell function prior to applying a fast Fourier transform. A lock mass of *m/z* 223.06345 (a polysiloxane) was used for online calibration. For the apodized data, the measured resolving power at *m/z* 200 was 300,000. Data were analyzed using DataAnalysis 4.2 (Bruker Daltonik GmbH, Bremen, Germany) in 10 minute time retention intervals with the first 10 minutes used for background subtraction. Assignments were made using Composer 1.5.7 (Sierra Analytics, Modesto, CA, USA), searching for homologous series within the elemental constraints C=0-200; H=0-1000; N=0-2; O=0-9; S=0-2; P=0-1 (Table S2). Aabel NG2 v.5.2 (Gigawiz Ltd. Co., Tulsa, Oklahoma, USA) was used for data visualization.

221

222

223

3. RESULTS AND DISCUSSION

3.1 ROCK-EVAL(6)PYROLYSIS

Inspection of the TOC content and its two major components, S1 and S2, at each sampling interval (Figure 2) shows a rapid decrease from surface to 25 cm, which may be due to the presence of natural extractable free hydrocarbon compounds and structural biopolymers in the rooting zone of living marsh plants (Newell et al., 2016). Below 25 cm depth the hydrocarbon content (TOC, S1, S2) was low and invariant with exception of a broad concentration peak at 47 - 49 cm and another at 79 - 81 cm (Figure 2). These were taken to indicate anthropogenic oil spills, possibly including the 1990 Exxon pipeline spill. Similarly, corresponding changes were also confirmed by the concentrations of residual carbon (RC %) (non-pyrolyzable) and production index (PI) (Figure 2). The latter parameter is a widely utilized by hydrocarbon explorationists to assess the amount of generated as compared to potential hydrocarbons. In this current work increasing PI values also appear to have considerable utility for the identification of possible hydrocarbon pollution events.

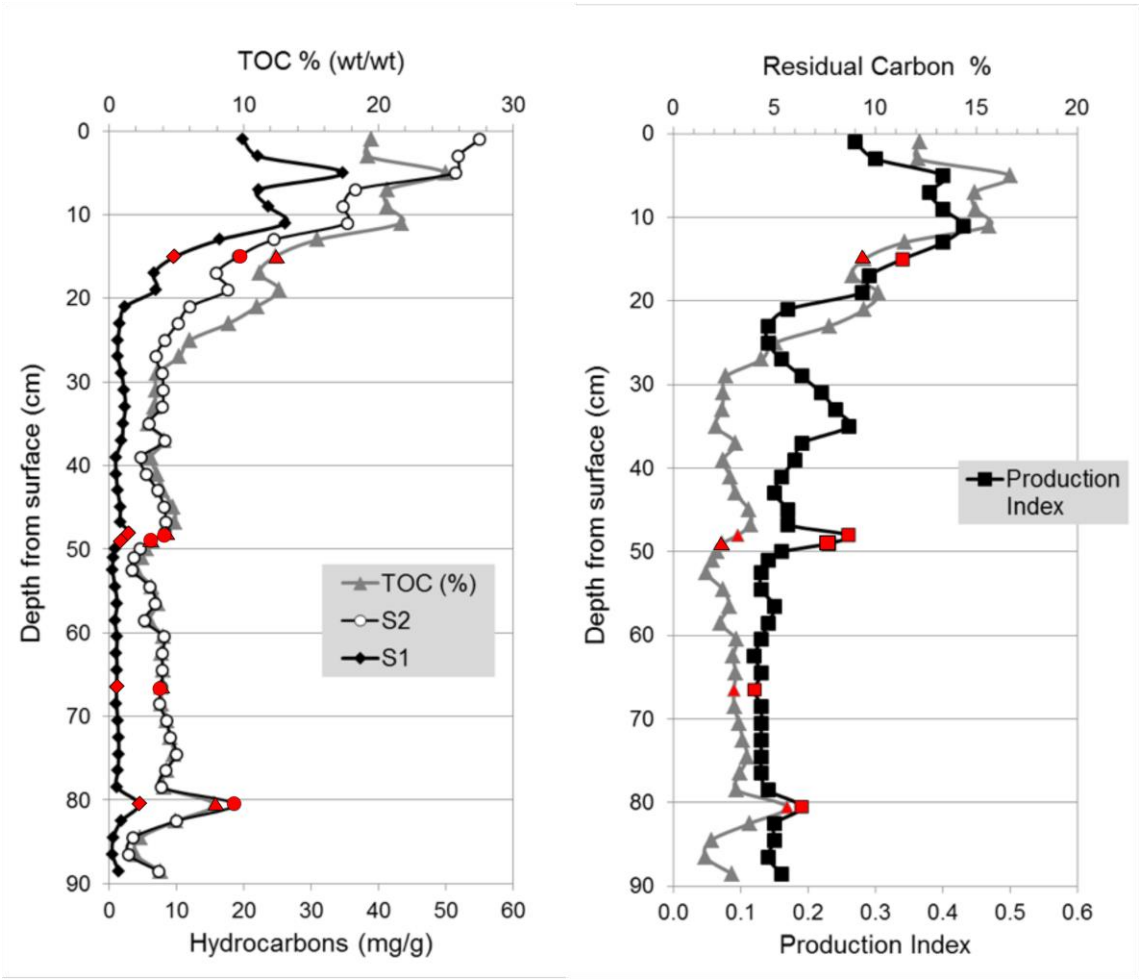

Figure 2. TOC and RC analysis by Rock-Eval(6) Pyrolysis

The key sampling depths carried forward for further analysis by FTICR MS methods are indicated by red markers in Figure 2, with 67.5 – 69.5 cm included as a sample with low PI for comparison.

3.2 DI-APPI FTICR MS

Broadband mass spectra were obtained for soil extracts, produced using soil samples originating from 5 depths, with the spectra shown in Figure 3. The mass distribution shifts between extract sampling depths, with 14 - 16 to 67.5 - 69.5 cm centred approximately on *m/z* 350, while 79.5 - 81.5 cm is centred on a higher *m/z* of 500 and has greater spectral intensity over the entire distribution.

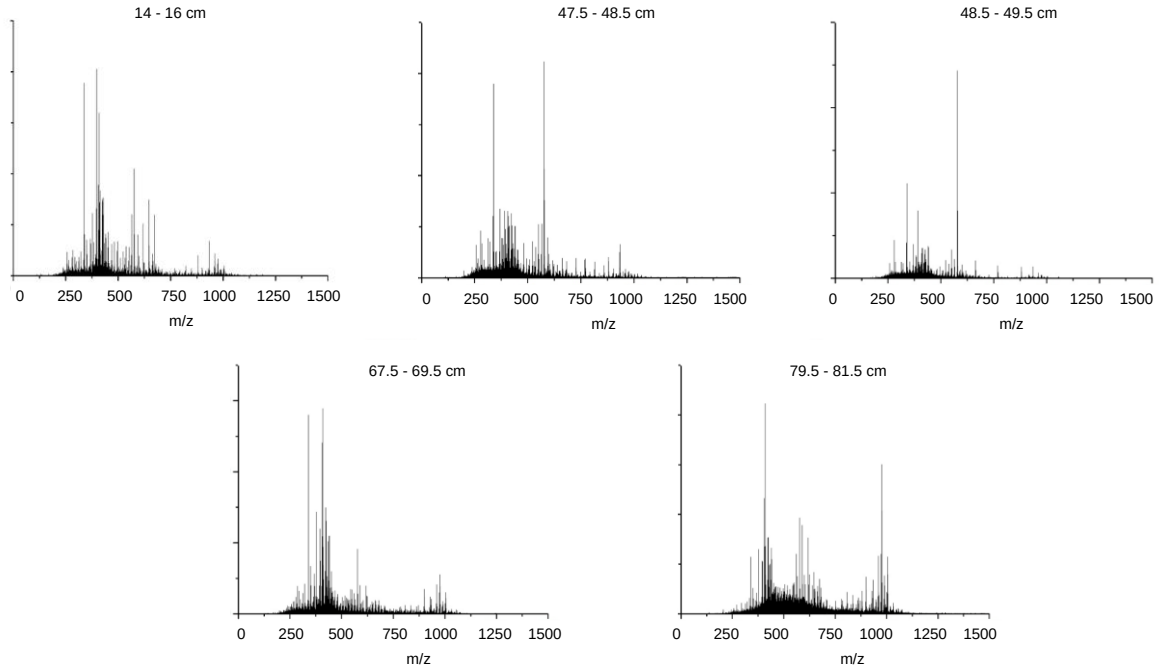

Figure 3. DI-APPI FTICR mass spectra for 5 sampling depths

MS data were analyzed by searching for homologous series of peaks separated by the CH_2 (14.01565 Da) repeat unit (Table S1). Homologous series of molecular formulae possess the same heteroatom content (compound class) and number of double bond equivalents (DBE) (McLafferty and Turecek, 1993) and increase incrementally with each CH_2 repeat unit by one carbon number (Marshall and Rodgers, 2008). A compound class distribution, showing the total relative intensity of peaks assigned to each compound class, is shown for all sampling depths in Figure 4.

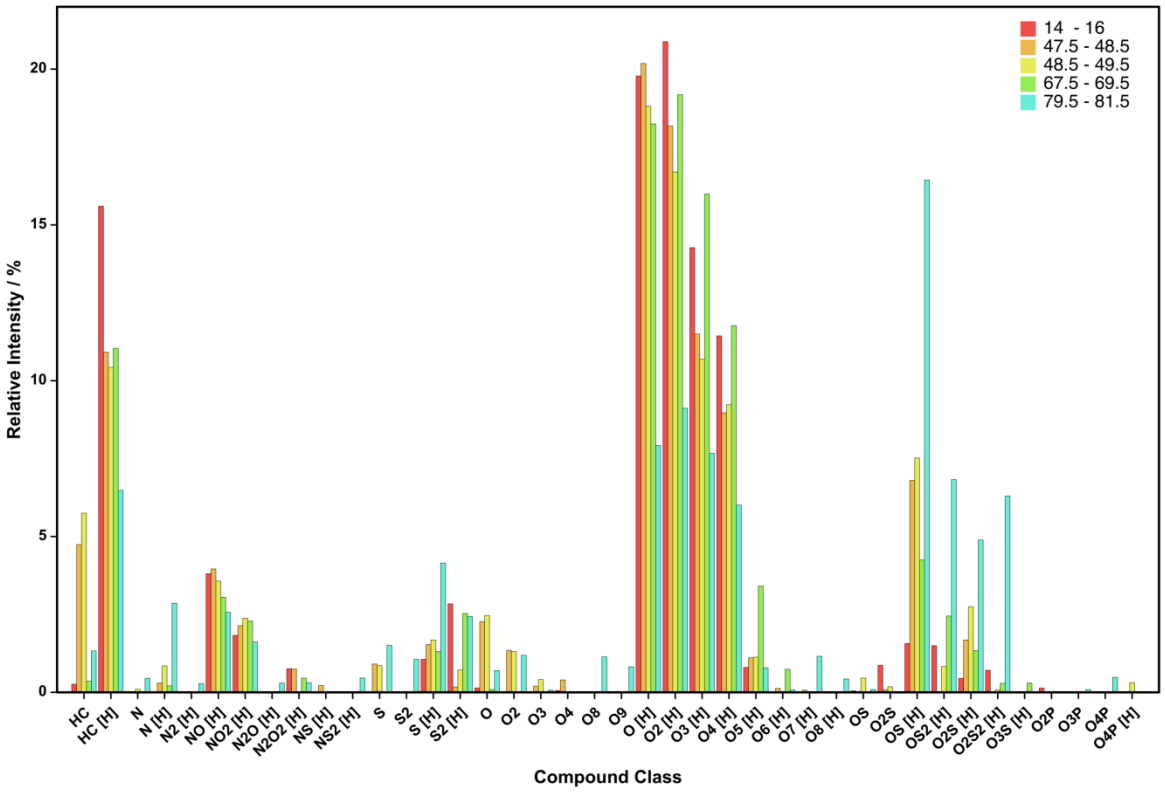

Figure 4. Compound class distribution for 5 sampling depths

Several key compositional differences between sampling depths are seen in Figure 4, particularly a sharp increase in the relative contribution from high oxygen containing O_x and O_xS_y[H] compounds, when moving from the shallower samples to the deepest sample at 79.5 - 81.5 cm. At the depths of 47.5 - 48.5 and 48.5 - 49.5 cm, there is a relatively strong contribution from the HC radical class, correlating well with the higher concentrations of free and bound hydrocarbons measured by Rock-Eval pyrolysis. The HC radical class most likely comprises polycyclic aromatic hydrocarbons (PAHs), as extensively condensed hydrocarbons can stabilise free radicals readily due to delocalisation throughout the aromatic framework (Creary et al., 1989). The depths of 47.5 - 48.5, 48.5 - 49.5 and 79.5 - 81.5 cm also have contributions from the N containing classes, commonly detected in petroleum-related mixtures, where the N[H] class typically corresponds to pyridinic species that protonate readily, while the N class often represents pyrrolic species that ionize by forming radical species (Tables S3 and S4).

The relative contribution from oxygenated and sulfur-containing radical classes was found to be greater at the sampling depths associated with a spike in PI. Inspection of the plots of number of rings and double bonds, or double bond equivalents (DBE), against carbon number (Figures S1-S3) for individual compound classes can provide information on the likely molecular structures of these compounds (Purcell et al., 2007a; Purcell et al., 2007b, Purcell et al., 2007c). Figure S1 shows that the S radical class of 47.5 - 48.5, 48.5 - 49.5 and 79.5 – 81.5 cm starts at 6 DBE and has higher intensities at DBEs of 9, 12, and 15, a pattern characteristic of thiophenic compounds (Hegazi et al., 2012; Hourani et al., 2013; Panda et al., 2007) that, due to their aromatic structure, form radical species during ionization. This is in contrast to the S_y[H] classes that comprise sulfur-containing groups that are more readily protonated during ionization, such as sulfides, which were detected at all depths and in the 79.5 – 81.5 cm sample at a relatively higher intensity. The differentiation between ion types for compositions with the same heteroatoms can be useful indications of differences in structure; the S[H] class begins at a lower DBE than the S radical class and does not have the characteristic pattern of higher intensities at DBE of 6, 9, 12, and 15 (Figure S2).

The increase in contribution from highly oxygenated O_x and O_xS_y classes may be linked to ageing of petroleum compounds (Atlas, 1981; Chen et al., 2016; Wang et al., 1998), and may be used to provide information of the timing of contamination due to particular spills (Douglas et al., 1996). Although geochemical tools can be used to more accurately date samples collected in areas with minimal sediment mixing, the samples used in this were collected at a site close to an active creek channel which in turn connects to the main tidal Arthur Kill waterway (a view supported by the changing sedimentology), and are therefore unlikely to provide an interpretable classical chronology (Vane et al., 2010; Vane et al., 2011). The DBE plots of the O_2S_1[H] class (Figure S3) show a higher DBE and carbon number range at two of the depths associated with a spike in PI, and greater relative intensities above DBE 5.5, which may be

298 partly due to oxygenation of benzothiopenic species, that, due to the incorporation of a polar
299 oxygen functionality, are more readily ionized by protonation (Fathalla, 2011; Griffiths et al.,
300 2014). O_xS_y[H] classes may represent sulfoxides, whereas the corresponding radical class
301 (O_xS_y) may have oxygen incorporated as aldehyde or ketone moieties in the hydrocarbon
302 backbone (Bobinger, 2009).

303 *3.3 GC-APCI FTICR MS*

304 The total ion chromatogram (TIC) is shown in Figure 5 for the 67.5 - 69.5 cm depth sample.
305 The average spectra taken over 10 minute time intervals of the TIC, show a shift in petroleum
306 distribution to higher *m/z* with increasing retention time. While 10 minute intervals represent a
307 relatively long period with respect to chromatography, they have been used here simply for the
308 purposes of data visualization to illustrate clear differences between the data corresponding to
309 the time ranges. Furthermore, coupling of GC to FTICR generates large data sets, necessitating
310 a trade-off between time resolved information and the amount of time required for data
311 analysis. It should be noted that the original, time-resolved information, such as extracted ion
312 chromatograms of individual ions, is retained with an example provided.

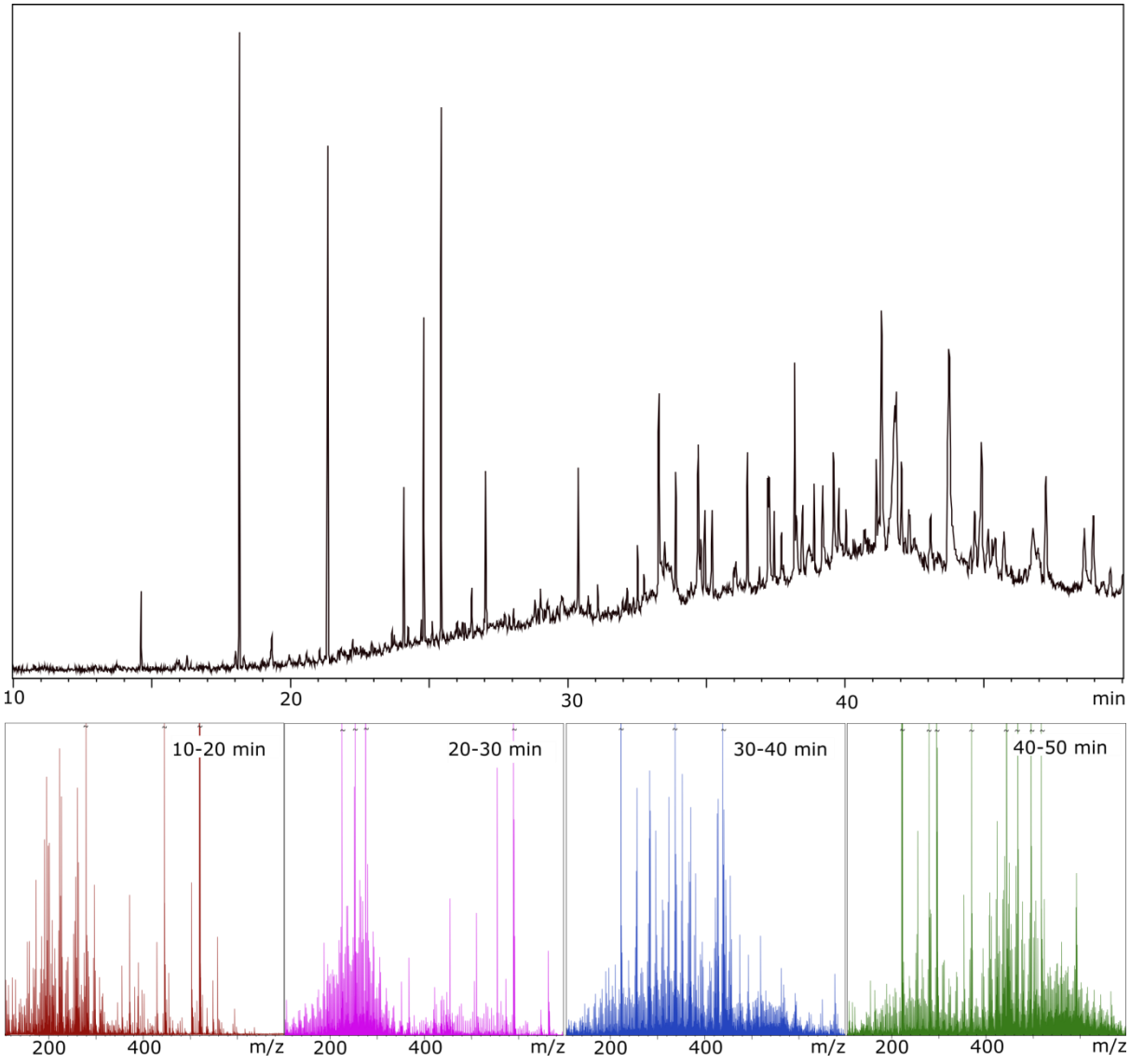

Figure 5. Total ion chromatogram for sampling depth 67.5 – 69.5 cm, which was found to have the lowest PI by Rock-Eval pyrolysis, and the mass spectra resulting from averaging the acquired scans over 10 minute intervals.

The compound class distribution shown in Figure 6 demonstrates that several heteroatom containing compound classes were observed at greater relative intensity when using GC-APCI FTICR MS compared to DI-APPI FTICR MS. The summed class distribution can be disseminated to the distributions observed over 10 minute intervals (Figure S4 – S7), further demonstrating that several classes were more readily observed by GC-APCI FTICR MS compared to DI-APPI FTICR MS measurements, including low intensity O_x and O_xP classes.

Although the N[H] class, typically comprising pyridinic species, is seen at a low relative intensity in all samples, in contrast to DI-APPI the N class, typically comprising pyrollic species (Purcell et al., 2007a; Purcell et al., 2007c), is not seen as readily, including in the 79.5 – 81.5 cm sample (Figure S7). The two techniques offer complimentary access to sample composition, due both to the differences in the volatility of compounds accessed by DI and GC and the differences in preferential ionization. While the differences in preferential ionization were not extensive when compared to methods such as ESI (Huba et al., 2016), APPI and APCI do offer some complementarity. 0.30 Da regions of mass spectra are shown in Figure S8, comparing a spectrum acquired using DI-APPI FTICR MS on a 12 T solariX instrument and a spectrum acquired using GC-APCI FTICR MS on a 7 T solariX 2XR instrument at the 40 - 50 min retention interval. Figure S8 shows not only the ultrahigh resolution capabilities of the 12 T and 7 T 2XR instruments, but also heteroatom class assignments common to both DI-APPI and GC-APCI methods, as well as unique molecular compositions in each case. DI-APPI provided a greater ionization response for polycyclic aromatic hydrocarbons and sulfur-containing species, while GC-APCI afforded greater access to more highly oxygenated compounds.

Notably, phosphorous-containing classes including $O_4P[H]$ also make a substantial contribution to the depths of 14 – 16 cm, 48.5 – 49.5 cm, and 67.5 - 69.5 cm (Figures S4 – S7), typically eluting early in the run. The $O_4P[H]$ class was also detected in DI-APPI FTICR MS experiments at 48.5 - 49.5 cm. Several possible sources of phosphorous contamination in the NY/NJ Estuary exist, including agricultural effluent, leaks from chemical plants and manufacturers, and leaching of materials dumped in the now closed Fresh Kills Landfill (Anon, 2001). Example phosphorous compounds detected by GC-APCI FTICR MS include $[C_8H_{19}O_4P + H]^+$ and $[C_{12}H_{27}O_4P + H]^+$ which may be dibutyl and tributyl phosphate,

substances that are used in multiple industrial processes and, in the latter case, in fungicides and herbicides (Thomas et al., 1997). It is of particular note that, in the initial screening provided by Rock-Eval pyrolysis, the sampling depth of 67.5 – 69.5 cm appeared to contain relatively low levels of both free volatile hydrocarbons and bound polymeric hydrocarbons, as indicated in Figure 2, but that DI-APPI and GC-APCI analyses show that soil at this depth contains a range of substances that may have an anthropogenic source, including shipping activity, refineries, industrial and agricultural chemicals, landfill leachate, and sewage which suggests that the NY/NJ Estuary is continually affected by contamination. Natural interferences in the analysis of an environmental complex mixture cannot be ruled out completely, although the extraction in DCM limits the hydrophilic substances, such as natural organic matter (Hertkorn et al., 2008), carried forward for FTICR MS.

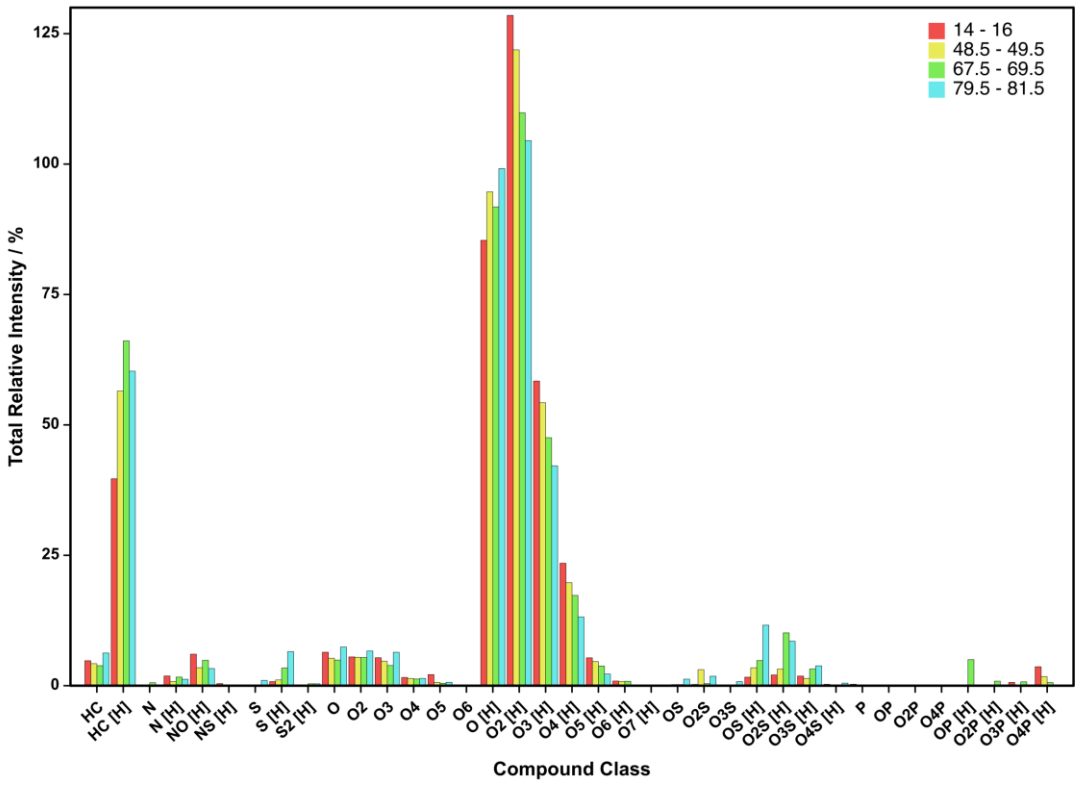

Figure 6. Compound class distribution from GC-APCI FTICR MS analysis of four sampling depths, summed over all retention time intervals.

Several compound classes elute preferentially at specific times, for example the relative contributions from the O_xS[H] classes generally increase with retention time. NO[H] and S[H] have the greatest relative intensity at 30 - 40 min at both the 14 - 16 cm and 67.5 – 69.5 cm sampling depths. The O_xP[H] classes have the greatest relative intensity at the early elution times of 10 - 20 and 20 - 30 min. A lower relative intensity of the S_1 class was seen for all samples by GC-APCI compared to DI-APPI, which may be associated with the greater ionization efficiency of more aromatic compounds by APPI. Figure S4 – S7 show a high relative contribution from the HC[H] class, which increases from the first time interval, and this corresponds to an increase in the number of data points as seen in the DBE plots shown in Figure 7a for the 67.5 – 69.5 cm sampling depth. Figure 7a also shows the DBE plots shifting to higher carbon number over time, with the highest mass species eluting later in the GC run. While there was an increase in absolute intensity for all DBE between 20 – 30 min and 40 – 50 min, Figure 7b shows the change in relative contribution from each DBE to the overall HC[H] class intensity. DBE of 2.5 and below, and 6.5 and above, make a greater relative contribution at 40 – 50 min, while those between 2.5 and 5.5 inclusive make a greater contribution at 20 – 30 min, suggesting that they have a lower boiling point due to weaker intermolecular attractions, and elute earlier as a result. An ion with DBE of 6.5 in the HC[H] class (neutral DBE of 7) corresponds to the threshold for two, fused, 6-membered, aromatic rings. By comparison, an ion DBE of 9.5 (neutral DBE of 10) corresponds to the threshold for the cata-condensed structure incorporating three, 6-membered, aromatic rings. As an additional example, the DBE plots for the O[H] class of the 14 – 16 cm sampling depth show a similar increase in carbon number and DBE over time (Figure S9a), but a more pronounced shift in the relative contribution from DBE of 6.5 and greater at 40 – 50 min compared to 20 - 30 min (Figure S9b).

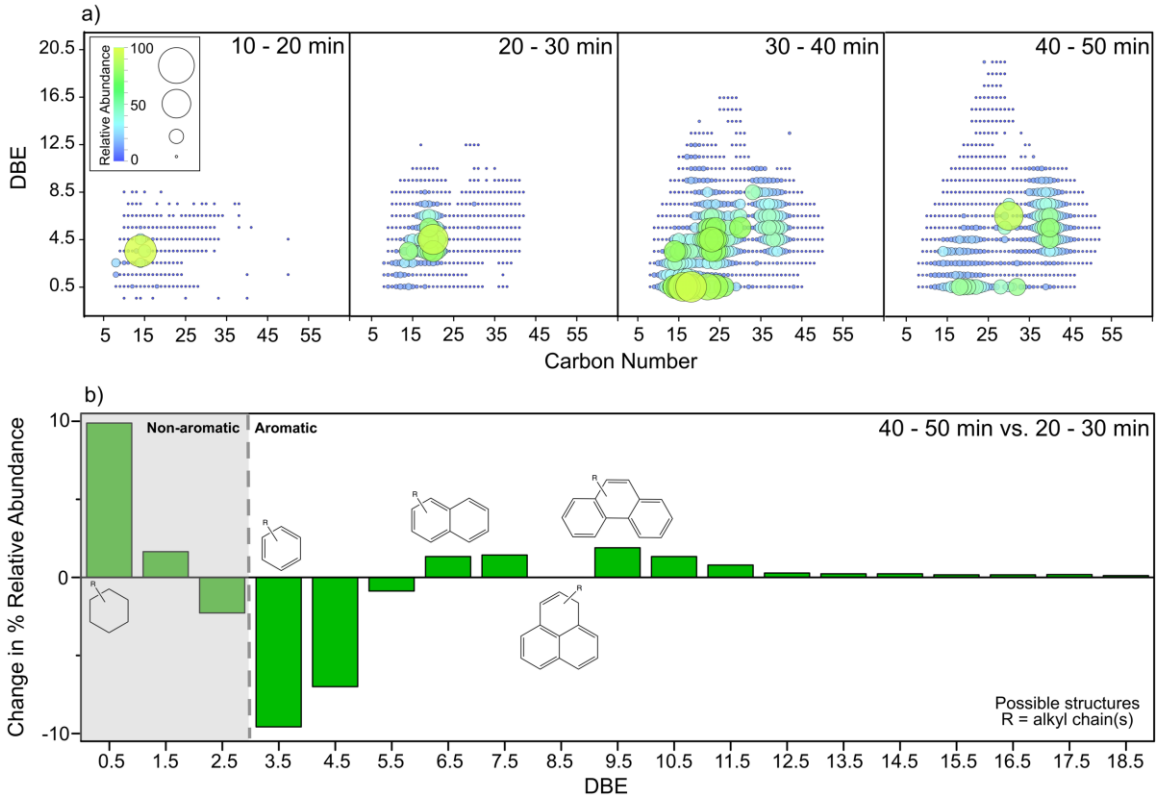

386

387 Figure 7. a) Plots of DBE against carbon number for the HC[H] class of sample depth 67.5 -
388 69.5 cm over 10 minute intervals of the GC-APCI FTICR MS experiment, where marker size
389 scales with relative intensity and b) Change in relative abundance of each DBE comparing the
390 40 - 50 min to the 20 - 30 min interval. Possible structures are shown for selected DBE values,
391 indicating where these specific structures would be found, if present.

392 DI-APPI was able to access a greater DBE range for the HC[H] class than GC-APCI, with
393 species detected up to a DBE of 25.5 (Figure S10). This can be explained by the preferential
394 ionization of aromatic structures offered by APPI, allowing extensively condensed PAHs to be
395 accessed more readily, as well as access to species with higher boiling points by DI. In contrast,
396 species with higher carbon numbers were accessed at the later elution times of GC-APCI,
397 including numerous assignments for carbon numbers in excess of 45.

398 Further adding to the complexity of the data, EICs can be used to visualise the number of
399 isomers present for a single molecular composition (data point) within a DBE plot. Figure 8

shows EICs for three individual molecular formulae, represented by three points on the DBE plot of the O[H] class (Figure S11). Figure 8 shows the additional depth and complexity of data offered by the coupled GC-APCI FTICR MS technique, with each molecular ion peak representative of multiple isomeric compounds, and increasing complexity when increasing both carbon number and DBE. The EICs span two or more of the 10 minute intervals over which averaged spectra were produced, demonstrating that information in the time dimension was not lost during data processing. By combining GC with the ultra-high resolving power of the FTICR MS instrumentation, the EICs are selected for a given molecular composition in a narrow window of ± 0.0005 Da, which would not be possible for an instrument operating at lower resolution. For instance, if the resolution at m/z 300 were 30,000 FWHM, this would limit the mass difference resolvable to 0.01 m/z, and selecting a peak with this window would result in the EICs for multiple molecular formulae detected in the study overlapping. In practice, peaks can be resolved to less than a ± 0.01 Da range within a GC-APCI mass spectrum in this study and, as a result, the EICs would overlap if this selection tolerance was used (Figure S12).

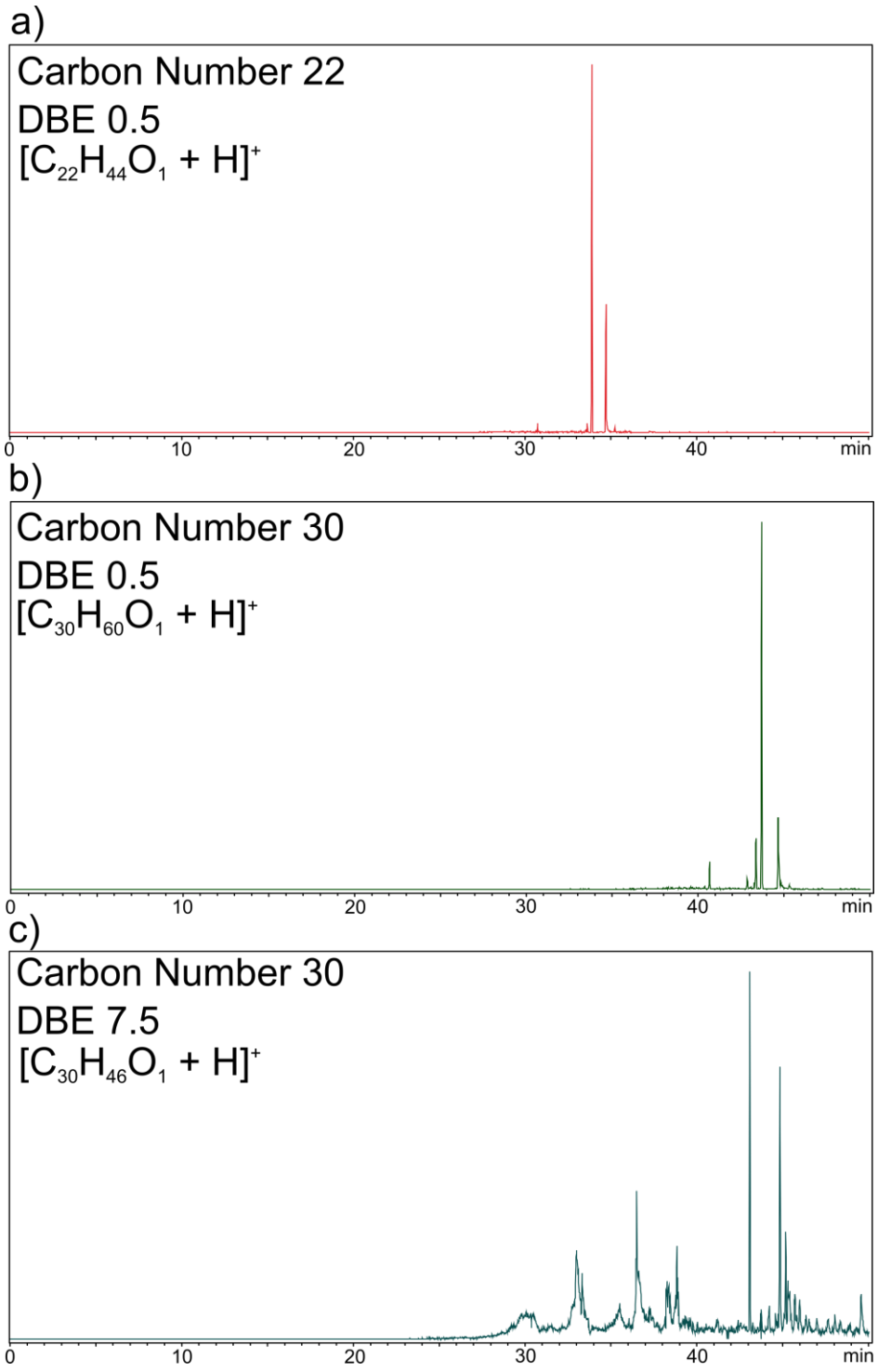

Figure 8. Extracted ion chromatograms for three individual molecular formulae from the O[H] class at 67.5 – 69.5 cm sampling depth, demonstrating increasing complexity with increasing carbon number and DBE (see Figure S11). b) represents an increase in carbon number from a), while c) represents an increase in DBE from b).

EICs can also be compared between sampling depths, providing an indication of the differences in isomeric complexity underlying relative class contributions and the range of structures possessing the same molecular formula (Figure 9). The EICs shown in Figures 8 and 9 demonstrate greater isomeric complexity for individual compositions than oil sands process water samples also studied by GC-APCI FT-ICR MS (Ortiz et al., 2014; Barrow et al., 2014), for example, although greater complexity may be determined utilising a chromatographic method not limited by boiling point, such as supercritical fluid chromatography (SFC) (Pereira and Martin, 2015) or high pressure liquid chromatography HPLC (Hawkes et al., 2018).

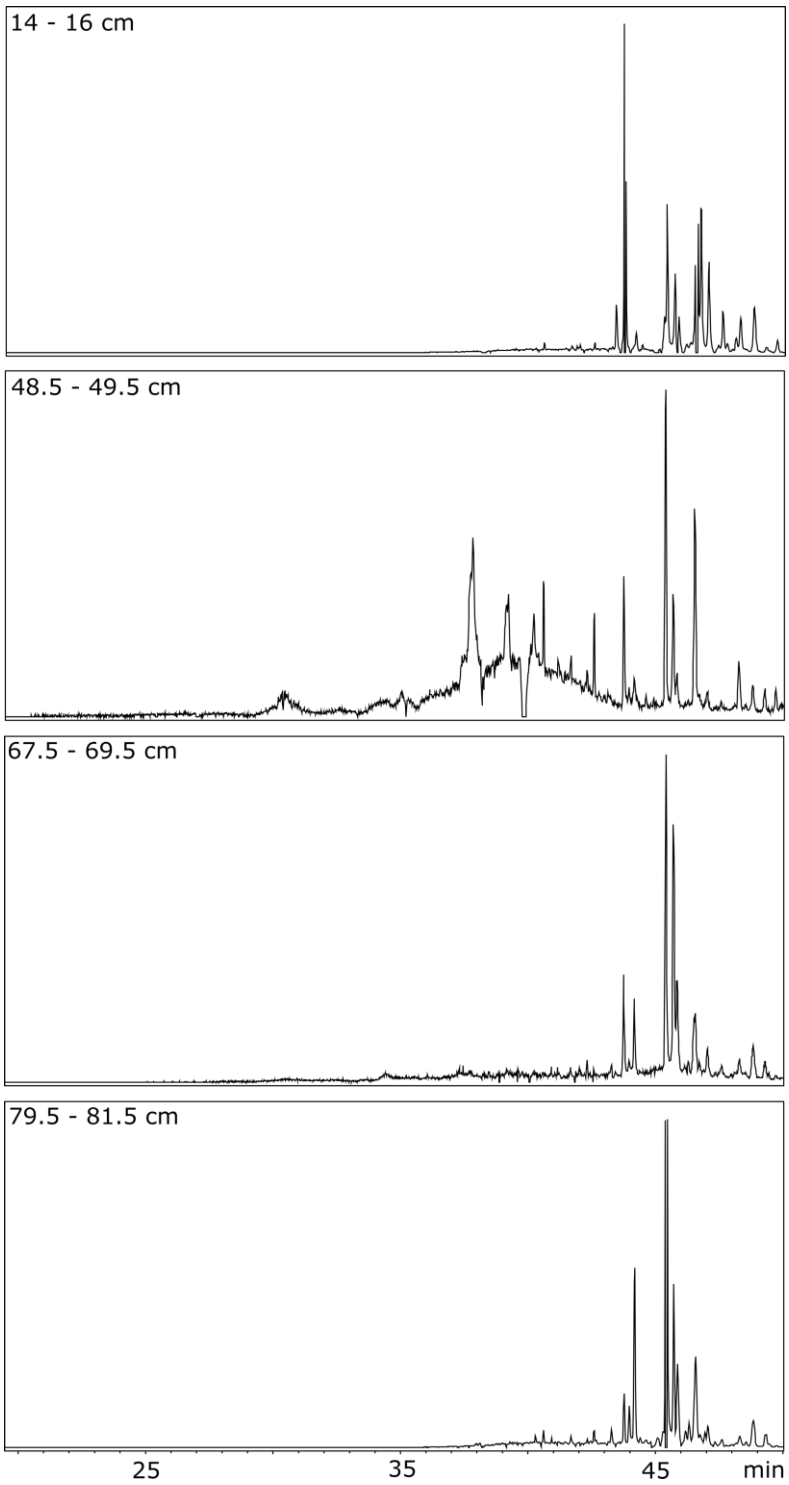

Figure 9. EICs for the molecular composition $[C_{30}H_{48} + H]^+$, demonstrating the differences in isomeric complexity and predominant retention times as a function of sampling depths.

4. CONCLUSION

Several sampling depths with relatively high PI were identified by bulk Rock-Eval pyrolysis, with key sampling depths that may be linked to major spills in the NY/NJ Estuary carried forward for further analysis. A sample with a relatively low PI was also included, as well as a sample representative of topsoil. To complement the Rock-Eval data obtained for these soil depths, the selected samples were profiled more extensively by DI-APPI FTICR MS, plus GC-APCI FTICR MS equipped with 2ω detection. Several trends in the compositional profile were observed by DI-APPI FTICR MS, including relatively high HC and O_xS_y[H] contributions, at the sampling depths that corresponded to a spike in PI by Rock-Eval analysis. The range of oxygen- and sulfur-containing classes observed increased at these depths, which may be related to contamination from petroleum-related compounds.

GC-APCI FTICR analysis identified additional groups and provided complementary information to DI-APPI data. Phosphorous-containing compounds with low retention times were detected, which may indicate contamination from other anthropogenic sources, including agricultural effluent and industrial chemicals, in the NY/NJ Estuary area. The sample that was found to have a relatively low PI by Rock-Eval pyrolysis was observed to contain many hydrocarbon and phosphorous-containing compounds by DI-APPI and GC-APCI FTICR MS, suggesting that there may have been continuous pollution from anthropogenic sources such as shipping, agricultural activity, refineries, and other industrial activity in the NY/NJ Estuary.

Finally, the 7 T solariX 2XR instrument was shown to be capable of providing ultrahigh resolution data comparable to that obtained at the higher field of 12 T on sufficiently short timescales suitable for coupling with GC. Coupling GC with ultrahigh resolution mass spectrometry affords a unique capability to resolve a greater number of compounds, including co-eluting components, making it possible to resolve EICs fully and to detect isomeric

components, even within highly complex mixtures. This provides greater analytical capabilities for complex mixture analysis and reduces the risk of loss of information which would result from coupling GC with lower resolution instruments. The viability of GC-APCI FTICR MS experiments on the 7 T 2XR instrument, using 2ω mode for increased performance, has been demonstrated as an emerging tool for the analysis of complex samples, including petroleum and environmental samples.

ACKNOWLEDGEMENTS

Mary J. Thomas thanks EPSRC for a PhD studentship through the EPSRC Centre for Doctoral Training in Molecular Analytical Science, grant number EP/L015307/1.

Diana Catalina Palacio Lozano and Mark P. Barrow would like to thank the Newton Fund award (reference number 275910721), Research Agreement No. 5211770 UIS-ICP, and COLCIENCIAS (project No. FP44842-039-2015).

The authors would also like to thank David Stranz, Sierra Analytics, for developments and access to Composer software, and Ana Milena Palacio (Universidad Nacional de Colombia, Palmira, Colombia) for assistance with the graphical abstract.

Christopher H. Vane and Vick Moss-Hayes publish with permission of the Executive Director, British Geological Survey (BGS).

DECLARATIONS OF INTEREST: None

APPENDIX A: SUPPLEMENTARY DATA

Supplementary data related to this article can be found at ___

REFERENCES

Alimi, H., Ertel, T., Schug, B., 2003. Fingerprinting of hydrocarbon fuel contaminants: Literature review. Environ. Forensics, 4:25-38.

Andrade, F. J., Shelley, J. T., Wetzel, W. C., Webb, M. R., Gamez, G., Ray, S. J., Hieftje, G. M., 2008. Atmospheric Pressure Chemical Ionization Source. 1. Ionization of Compounds in the Gas Phase. Anal. Chem., 80:2646-2653.

Anonymous, 2001. New York, New York - Fresh kills landfill closes. BioCycle, 42:22-23.

Atlas, R. M., 1981. Microbial-Degradation Of Petroleum-Hydrocarbons - An Environmental Perspective. Microbiol. Rev., 45:180-209.

Barrow, M. P., 2010. Petroleomics: study of the old and the new. Biofuels, 1:651-655.

Barrow, M. P., Peru, K. M., Headley, J. V., 2014. An Added Dimension: GC Atmospheric Pressure Chemical Ionization FTICR MS and the Athabasca Oil Sands. Anal. Chem., 86:8281-8288.

Barrow, M. P., Witt, M., Headley, J. V., Peru, K. M., 2010. Athabasca Oil Sands Process Water: Characterization by Atmospheric Pressure Photoionization and Electrospray Ionization Fourier Transform Ion Cyclotron Resonance Mass Spectrometry. Anal. Chem., 82:3727-3735.

Beens, J., Brinkman, U., 2000. The role of gas chromatography in compositional analyses in the petroleum industry. TrAC, Trends Anal. Chem., 19:260-275.

Benigni, P., DeBord, J., Thompson, C., Gardinali, P., Fernandez-Lima, F., 2016. Increasing Polyaromatic Hydrocarbon (PAH) Molecular Coverage during Fossil Oil Analysis by Combining Gas Chromatography and Atmospheric-Pressure Laser Ionization Fourier Transform Ion Cyclotron Resonance Mass Spectrometry (FT-ICR MS). Energy Fuels, 30:196-203.

Beriro, D. J., Vane, C. H., Cave, M. R., Nathanail, C. P., 2014. Effects of physical sample preparation on the concentrations of polycyclic aromatic hydrocarbons in gasworks contaminated soils. Chemosphere, 111:396-404.

Blomberg, J., Schoenmakers, P. J., Brinkman, U. A. T., 2002. Gas chromatographic methods for oil analysis. J. Chromatogr. A, 972:137-173.

Boldin, I. A., Nikolaev, E. N., 2011. FTICR cell with dynamic harmonization of the electric field in the whole volume by shaping of excitation and detection electrode assembly. Rapid Commun. Mass Spectrom., 25:122-126.

Cho, E., Witt, M., Hur, M., Jung, M.-J., Kim, S., 2017. Application of FT-ICR MS Equipped with Quadrupole Detection for Analysis of Crude Oil. Anal. Chem., 89:12101-12107.

Chen, H., Hou, A. X., Corilo, Y. E., Lin, Q. X., Lu, J., Mendelssohn, I. K., Zhang, R., Rodgers, R. P., McKenna, A. M., 2016. 4 Years after the Deepwater Horizon Spill: Molecular Transformation of Macondo Well Oil in Louisiana Salt Marsh Sediments Revealed by FT-ICR Mass Spectrometry. Environ. Sci. Technol., 50:9061-9069.

Cho, Y., Ahmed, A., Islam, A., Kim, S., 2015. Developments in FT-ICR MS instrumentation, ionization techniques, and data interpretation methods for petroleomics. Mass Spectrom. Rev., 34:248-263.

Cho Y., Mi J. J., Witt M., Birdwell J. E., Na J. G., Roh N. S., Kim, S., 2013. Comparing laser desorption ionization and atmospheric pressure photoionization coupled to Fourier transform ion cyclotron resonance mass spectrometry to characterize shale oils at the molecular level. Energy Fuels, 27:1830–1837.

Creary, X., Mehrsheikh-Mohammadi, M. E., McDonald, S., 1989. A Comparison of the Radical-Stabilizing Ability of Aromatic Groups. γ• Values for Aromatic Groups. J. Org. Chem., 54, 2904-2910.

da Silva, D. A. M., Bicego, M. C., 2010. Polycyclic aromatic hydrocarbons and petroleum biomarkers in Sao Sebastiao Channel, Brazil: Assessment of petroleum contamination. Mar. Environ. Res., 69:277-286.

Douglas, G. S., Bence, A. E., Prince, R. C., McMillen, S. J., Butler, E. L., 1996. Environmental stability of selected petroleum hydrocarbon source and weathering ratios. Environ. Sci. Technol., 30:2332-2339.

Fathalla., E. M., 2011. Products of Polycyclic Aromatic Sulfur Heterocycles in Oil Spill Photodegradation. Environ. Toxicol. Chem., 30:2004 - 2012.

Griffiths, M. T., Da Campo, R., O'Connor, P. B., Barrow, M. P., 2014. Throwing light on petroleum : simulated exposure of crude oil to sunlight and characterization using atmospheric pressure photoionization fourier transform ion cyclotron resonance mass spectrometry. Anal. Chem., 86:527-534.

Gunster, D. G., Gillis, C. A.; Bommevie, N. L., Abel, T. B., Wenning, R. J., 1993. Petroleum and hazardous chemical spills in Newark Bay, New Jersey, USA from 1982 to 1991. Environ. Pollut., 82:245-253.

Hawkes, J. A., Patriarca, C., Sjöberg, P. J. R., Tranvik, L. J., Bergquist, J., 2018. Extreme isomeric complexity of dissolved organic matter found across aquatic environments. Limnol. Oceanogr. Lett., 3:21-30.

Headley, J. V., Barrow, M. P., Peru, K. M., Fahlman, B., Frank, R. A., Bickerton, G., McMaster, M. E., Parrott, J., Hewitt, L. M., 2011. Preliminary fingerprinting of Athabasca oil sands polar organics in environmental samples using electrospray ionization Fourier transform ion cyclotron resonance mass spectrometry. Rapid Commun. Mass Spectrom., 25:1899-1909.

Hegazi, A. H., Fathalla, E. M., Panda, S. K., Schrader, W., Andersson, J. T., 2012. High-molecular weight sulfur-containing aromatics refractory to weathering as determined by Fourier transform ion cyclotron resonance mass spectrometry. Chemosphere, 89:205-212

Hertkorn, N., Frommberger, M., Witt, M., Koch, B. P., Schmitt-Kopplin, P., Perdue, E. M., 2008. Natural organic matter and the event horizon of mass spectrometry. Anal. Chem., 80:8908-8919.

Hourani, N., Andersson, J. T., Möller, I., Amad, M., Witt, M., Sarathy, S. M., 2013. Atmospheric pressure chemical ionization Fourier transform ion cyclotron resonance mass spectrometry for complex thiophenic mixture analysis. Rapid Commun. Mass Spectrom., 27:2432–2438.

Hsu, C., Hendrickson, C., Rodgers, R., McKenna, A., Marshall, A., 2011. Petroleomics: advanced molecular probe for petroleum heavy ends. J. Mass Spectrom., 46:337-343.

Huba, A. K., Huba, K., Gardinali, P. R., 2016. Understanding the atmospheric pressure ionization of petroleum components: The effects of size, structure, and presence of heteroatoms. Sci. Total Environ., 568:1018-1025.

Jertz, R., Friedrich, J., Kriete, C., Nikolaev, E. N., Baykut, G., 2015. Tracking the Magnetron Motion in FT-ICR Mass Spectrometry, J. Am. Soc. Mass Spectrom., 26:1349-1366.

Lalli, P. M., Jarvis, J. M., Marshall, A. G., Rodgers, R. P., 2017. Functional Isomers in Petroleum Emulsion Interfacial Material Revealed by Ion Mobility Mass Spectrometry and Collision-Induced Dissociation. Energy Fuels, 31:311-318.

603 Langston, W. J., O'Hara, S., Pope, N. D., Davey, M., Shortridge, E., Imamura, M., Harino, H.,
604 Kim, A. W., Vane C. H., 2012. Bioaccumulation surveillance in Milford Haven Waterway.
605 Environ. Monit. Assess., 184:289-311.
606
607 Könitzer, S. F., Stephenson, M. H., Davies, J., Vane, C. H., Leng, M. J., 2016. Significance of
608 sedimentary organic matter input for shale gas generation potential of Mississippian
609 Mudstones, Widmerpool Gulf, UK. Rev. Palaeobot. Palynol., 224:146-148.
610
611 Marshall, A., Blakney, G., Beu, S., Hendrickson, C., McKenna, A., Purcell, J., Rodgers, R.,
612 Xian, F., 2010. Petroleomics: a test bed for ultra-high-resolution Fourier transform ion
613 cyclotron resonance mass spectrometry. Eur. J. Mass Spectrom., 16:367-371.
614 Marshall, A., Rodgers, R., 2008. Petroleomics: Chemistry of the underworld. Proc. Natl. Acad.
615 Sci. U. S. A., 105:18090-18095.
616
617 McLafferty, F. W., Turecek, F., 1993. Interpretation of Mass Spectra. 4 ed.; University Science
618 Books: Mill Valley, CA.
619
620 Newell, A. J., Vane, C. H., Sorensen, J. P. R., Moss-Hayes, V., Gooddy, D. C., 2016. Long-
621 term Holocene groundwater fluctuations in a chalk catchment: evidence from Rock-Eval
622 pyrolysis of riparian peats. Hydrol. Processes, 30:4556-4567
623
624 Oros, D. R., Ross, J. R. M., 2004. Polycyclic aromatic hydrocarbons in San Francisco Estuary
625 sediments. Mar. Chem., 86:169-184.
626

627 Packer, D. B., 1991 NOAA Technical Memorandum NMFS-NE-167. Assessment of
628 characterisation of salt marshes in the Arthur Kill (New York-New Jersey) replanted after a
629 server oil spill. pp. 232.
630
631 Pan, Y., Ridge, D. P., Rockwood, A. L., 1988. Harmonic Signal Enhancement in ion-cyclotron
632 resonance mass-spectrometry using Multiple Electrode Detection. Int. J. Mass Spectrom. Ion
633 Processes, 84:293-304.
634
635 Panda, S. K., Schrader, W., al-Hajji, A., Andersson, J. T., 2007. Distribution of Polycyclic
636 Aromatic Sulfur Heterocycles in Three Saudi Arabian Crude Oils as Determined by Fourier
637 Transform Ion Cyclotron Resonance Mass Spectrometry. Energy Fuels, 21: 1071-1077.
638
639 Pereira, A. S., Martin, J. W., 2015. Exploring the complexity of oil sands process- affected
640 water by high efficiency supercritical fluid chromatography/orbitrap mass spectrometry. Rapid
641 Commun. Mass Spectrom., 29:735-744.
642
643 Pharaoh T. C., Gent, M. A., Hannis, S. D., Kirk, K. L., Monaghan, A. A., Quinn, M. F., Smith,
644 N. J. P., Vane, C. H., Wakefiled, O., Waters, C. N., 2018. An overlooked play? Structure,
645 stratigraphy and hydrocarbon prospectivity of the Carboniferous in the East Irish Sea-North
646 Channel basin complex. Geol. Soc. Spec. Publ., 471.
647
648 Purcell, J. M., Hendrickson, C. L., Rodgers, R. P., Marshall, A. G., 2007a. Atmospheric
649 Pressure Photoionization Proton Transfer for Complex Organic Mixtures Investigated by
650 Fourier Transform Ion Cyclotron Resonance Mass Spectrometry. J. Am. Soc. Mass Spectrom.,
651 18:1682-1689.

Purcell, J. M., Juyal, P., Kim, D.-G., Rodgers, R. P., Hendrickson, C. L., Marshall, A. G., 2007b. Sulfur Speciation in Petroleum: Atmospheric Pressure Photoionization or Chemical Derivatization and Electrospray Ionization Fourier Transform Ion Cyclotron Resonance Mass Spectrometry, Energy Fuels, 21:2869-2874.

Purcell, J. M., Rodgers, R. P., Hendrickson, C. L., Marshall, A. G., 2007c. Speciation of Nitrogen Containing Aromatics by Atmospheric Pressure Photoionization or Electrospray Ionization Fourier Transform Ion Cyclotron Resonance Mass Spectrometry. J. Am. Soc. Mass Spectrom., 18:1265-1273.

Richardson, S. D., Ternes, T. A., 2018. Water Analysis: Emerging Contaminants and Current Issues. Anal. Chem., 90:398-428.

Rowland, S. M., Robbins, W. K., Marshall, A. G., Rodgers, R. P., 2014. Characterization of Highly Oxygenated and Environmentally Weathered Crude Oils by Liquid Chromatography Fourier Transform Ion Cyclotron Mass Spectrometry (FT-ICR MS). International Oil Spill Conference Proceedings, 2014:300205.

Schweikhard, L., 1991. Theory of Quadrupole Detection Fourier transform ion cyclotron-resonance. Int. J. Mass Spectrom. Ion Processes, 107:281-292.

Schweikhard, L., Lindinger, M., Kluge, H. J., 1990. Quadrupole-detection FT-ICR mass-spectrometry. Int. J. Mass Spectrom. Ion Processes, 98:25-33.

677 Schwemer, T., Rüger, C. P., Sklorz, M., Zimmermann, R., 2015. Gas Chromatography Coupled
678 to Atmospheric Pressure Chemical Ionization FT-ICR Mass Spectrometry for Improvement of
679 Data Reliability. Anal. Chem., 87:11957-11961.
680
681 Slowakiewicz, M., Tucker, M. E., Vane, C. H., Harding, R., Collins, A., Pancost, R.D., 2015.
682 Shale-gas potential of the mid-Carboniferous Bowland-Hodder unit in the Cleveland Basin
683 (Yorkshire), Central Britain. J. Pet. Geol., 38:59-76.
684
685 Tessarolo, N. S., Silva, R. C., Vanini, G., Pinho, A., Romao, W., de Castro, E. V. R., Azevedo,
686 D. A., 2014. Assessing the chemical composition of bio-oils using FT-ICR mass spectrometry
687 and comprehensive two-dimensional gas chromatography with time-of-flight mass
688 spectrometry. Microchem. J., 117:68-76.
689
690 Thomas, R. A. P., Morby, A. P., Macaskie, L. E. The biodegradation of tributyl phosphate by
691 naturally occurring microbial isolates. FEMS Microbiol. Lett., 155:155-159.
692
693 Vane, C. H., Chenery, S. R., Harrison, I., Kim, A. W., Moss-Hayes, V., Jones, D. G., 2011.
694 Chemical signatures of the Anthropocene in the Clyde Estuary, UK: Sediment hosted Pb,
695 $^{207/206}$Pb, Polyaromatic Hydrocarbon (PAH) and Polychlorinated Biphenyl (PCB) pollution
696 records. Philos. Trans. R. Soc., A, 369:1085-1111
697
698 Vane, C. H., Harrison, I., Kim, A. W., 2007. Polycyclic aromatic hydrocarbons (PAHs) and
699 polychlorinated biphenyls (PCBs) in sediments from the Mersey Estuary, U.K. Sci. Total
700 Environ., 374:112-126.
701

Vane, C. H., Harrison, I., Kim, A. W., Moss-Hayes, V., Vickers, B. P., Hong, K., 2009. Organic and Metal Contamination in Surface Mangrove Sediments of South China. Mar. Pollut. Bull., 58:134-144.

Vane, C. H., Harrison, I., Kim, A. W., Moss-Hayes, V., Vickers, B. P., Horton., B. P., 2008. Status of Organic Pollutants in Surface Sediments of Barnegat Bay-Little Egg Harbor Estuary, New Jersey, USA. Mar. Pollut. Bull., 56:1802-1808.

Vane, C. H., Kim, A. W. McGowan, S., Leng, M. J., Heaton, T. H. E. Coombs, P. Kendrick, C. P., Yang, H., Swann, G. E. A., 2010. Sedimentary record of sewage pollution using faecal marker compounds in contrasting peri-urban shallow lakes. Sci. Total Environ., 409: 345-356.

Vane, C. H., Moss-Hayes, V., Kim, A. W., Edgley, E., Bearcock, J., 2018. Mercury (Hg), *n*-alkane and unresolved complex mixture (UCM) hydrocarbon pollution in surface sediment across rural-urban-estuarine continuum of the Clyde, UK. Earth Environ. Sci. Trans. R. Soc. Edinburgh (accepted in-press).

Wang, Z., Fingas, M., 1997. Developments in the analysis of petroleum hydrocarbons in oils, petroleum products and oil-spill-related environmental samples by gas chromatography. J. Chromatogr. A, 774:51-78.

Wang, Z. D., Fingas, M., Blenkinsopp, S., Sergy, G., Landriault, M., Sigouin, L., Foght, J., Semple, K., Westlake, D. W. S., 1998. Comparison of oil composition changes due to biodegradation and physical weathering in different oils. J. Chromatogr. A, 809:89-107.

White, H. K., Xu, L., Hartmann, P., Quinn, J. G., Reddy, C. M., 2013. Unresolved Complex Mixture (UCM) in Coastal Environments Is Derived from Fossil Sources. Environ. Sci. Technol., 47:726-731.

Zubair, A., Pappoe, M., James, L., Hawboldt, K., 2015. Development, optimization, validation and application of faster gas chromatography - flame ionization detector method for the analysis of total petroleum hydrocarbons in contaminated soils. J. Chromatogr. A, 1425:240-248.